CHAPTER 6

Multinuclear and Solid State NMR of Gels

Nonappa,[a,b]* and E. Kolehmainen[c]

[a] Aalto University, Department of Applied Physics, Puumiehenkuja 2, Espoo, 02150, Finland

[a] Aalto University, Department of Bioproducts and Biosystems, Kemistintie 1, Espoo, 02150, Finland

[b] Jyväskylä University, Department of Chemistry, Survontie 9, FI-40014, Jyväskylä, Finland

*Corresponding contributor. E-mail: nonappa@aalto.fi

CHAPTER **6**

Multinuclear and Solid State NMR of Gels

Table of Contents

Abstract

Over the past six decades, nuclear magnetic resonance spectroscopy has been an integral part of organic synthetic and organometallic chemistry, as well as biochemistry. Beyond solution state experiments, increasing developments have opened new avenues to study materials in their solid state. Between two extremes (i.e., solution and solid), there exist several other forms of materials, especially soft materials such as gels and liquid crystals. Traditionally gels have been studied using solution state NMR spectroscopic methods. However, the viscosity of complex viscoelastic fluids such as gels affects the molecular tumbling, which in turn affects the chemical shift anisotropy, dipolar and quadrupolar interactions resulting in broad spectral lines. Therefore, the importance of solid state (SS) NMR in understanding the structural details of self-assembled soft materials remained unexplored for several decades. Nevertheless, promising results in understanding weak interactions in polymer gels have been explored using solid state cross polarization (CP) and high resolution (HR) magic angle spinning (MAS) NMR spectroscopy. However, similar studies and the possibilities to utilized SS NMR spectroscopy to study hydro-, and organogels derived from low molecular weight gelators has been limited until recently. In this chapter, we will focus on the application of SS NMR to study xerogels, aerogels and native gels with selected examples.

6.1 Introduction

6.1.1 Molecular gels

Molecular self-assembly has emerged as a fascinating tool to construct structurally and functionally diverse soft materials across length scales.[1,2] Among self-assembled materials, molecular organo- and hydrogels represent a rapidly evolving area in soft matter science.[3-9] Molecular gels are also referred to as physical gels or supramolecular gels. Unlike covalently cross-linked polymer gels, the molecular gels involve low molecular weight organic molecules (LMOGs, Mw < 3 kDa) as their basic building blocks. Therefore, similar to other types of gels, molecular gels also contain continuous liquid component, and microphase separated gelator molecule.[10] Structurally and functionally diverse organic molecules ranging from fatty acids,[11] peptides,[12] carbohydrate derivatives,[13] steroids,[14] and urea derivatives[15] have been shown to undergo self-assembly directed by various non-covalent interactions. The non-covalent interactions include London dispersion forces, van der Waals interactions, π-stacking, hydrogen bonding, charge transfer complexation, and more recently, halogen bonding and metal coordination have been pursued to design novel functional gels.[16-22] Their remarkable ability to form highly entangled self-assembled fibrillar networks (SAFINs) and encapsulate a large amount of solvent makes them attractive candidates for potential applications in tissue engineering, catalysis, sensors, optoelectronics, and hybrid nanomaterials.[23] In polymer gels, the fundamental building blocks for three-dimensional networks are 1D objects. In contrast, the basic building blocks in low molecular gels are zero-dimensional molecular components, which self-assemble into high aspect ratio 1D structures (e.g., fibers, tapes, ribbons, etc.). These 1D structures then non-covalently crosslink to form highly entangled 3D networks.

A molecular gel is considered as a kinetically trapped, metastable state and the gelation process can be controlled by tuning the interactions and self-assembly pathways to obtain different material properties.[24] Further, different kinetically trapped gels can evolve into the same final gel state by overcoming the kinetic barriers, for examples by thermal treatment.[25] Therefore, one could say that the gels may also represent thermodynamic minima, that can be accessed reversibly. Gelation of small molecules has often considered as a failed crystallization, and recent reports have shown that there is a delicate balance between gelation and crystallization.[26] It has been shown that this balance between gel state and the crystallization that depends on the activation barrier. This is attributed to the fact that the formation of 3D structures such as crystals allows maximum stabilizing interactions compared to that of 1D structures found in the gels. However, in some cases, such as the peptide amphiphiles, the formation of 1D structures are inherently thermodynamically stable, such as peptide amphiphiles.[27] Molecular gels display other interesting features in their mechanical properties when studied under oscillatory rheology. Despite having an extremely small concentration of solid content, they display solid-like rheological properties. Molecular gels show higher storage modulus (G′) compared to the loss modulus (G′′) over a large frequency range.[10]

6.1.2 Characterization of gels

Despite the diversity in the structure and functionalities of the low molecular weight gelators, it has been demonstrated that gelation is due to self-assembled fibrillar networks (SAFINs) of gelators. However, it should be noted that there are other types of assemblies/ structures are known to form gel networks.[10] The presence of nanostructures in the gels are studied with various microscopy techniques not always in their native state. Majority of the cases either xerogels (dried gels), aerogels (i.e., freeze dried/lyophilized or using supercritical carbon dioxide) are used for electron microscopy. For hydrogels, shreds of evidence for the presence of fibrillar network structure in the hydrated state have been investigated using cryogenic transmission electron microscopy (Cryo-TEM).[28] Further, environmental scanning electron microscopy (ESEM),[29] atomic force microscopy (AFM),[30] critical point drying using supercritical carbon dioxide, and liquid propane freeze drying also offer possibilities to observe the structures close to their native state.[31,32] However, the microscopy techniques allow morphological features, but they involve various sample preparation, pre-treatment and imaging conditions, where the samples undergo severe changes or even damage. Though a wide variety of the gelators fail to produce quality single crystals, still, in some case, successful crystallization has been achieved.[33]. Therefore, the single crystal X-ray diffraction remains the most important tool for the evaluation of the nature of supramolecular interactions in the solid state. Further, in some cases, the SAFINs are shown to be microcrystalline, thus suggesting a certain degree crystallinity suitable for X-ray powder diffraction (XRPD) analysis.[34] While crystallization conditions often differ from the gelation, X-ray powder diffraction require dried gels (xerogel) or aerogels. Therefore, limited information is available for gels in their native state. In solution and gel state small-angle, X-ray scattering (SAXS) and small angle neutron scattering (SANS) analysis have been used to gain insight on the self-assembled superstructures.[35,36] However, there exist several challegnes to study amorphous materials, powder samples, polymers, and soft materials.

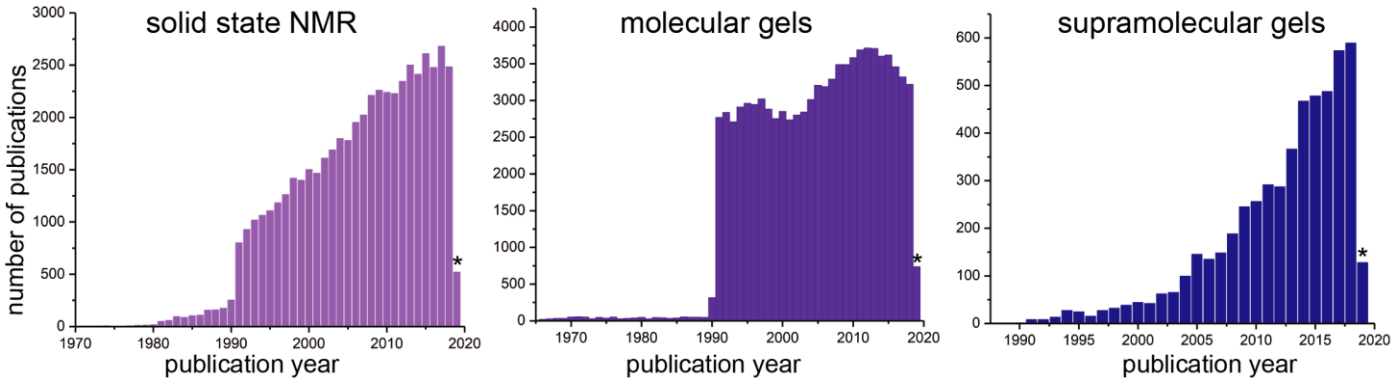

Figure 6.1. The number of publications vs. year using keywords, solid state NMR, molecular gels and supramolecular gels as entered in the web of science as of 20.03.2019. *indicates numbers for 2019 are incomplete.

Among, non-invasive analytical tools, solution state NMR spectroscopy methods have played a dominant role in the structural characterization of organic, inorganic, hybrids, macromolecular structures, biomolecules, and even single cells.[37,38] More importantly, the idea of using nuclear magnetic polarization to study crystalline solids has been implemented soon after its invention.[39] Continued progress in the field of NMR spectroscopy, solid state (SS) cross polarization (CP) and high resolution (HR) magic angle spinning (MAS), have made SS NMR an important tool in structural chemistry, material science, and biology.[40-46] SS NMR spectroscopy also offer possibilities to study non-crystalline materials, amorphous solids, liquid crystalline materials, gels and even living cells.[47-49] SS NMR can distinguish the presence of more than one of different polymorphs, conformational isomers present in a given system. Furthermore, using SS NMR one could readily extract the information related to the number of non-equivalent molecules present in an asymmetric unit of the crystal lattice. Therefore, SS NMR is considered as a complementary tool to X-ray diffraction.[50-56] The non-destructive and non-invasive nature of the experimental NMR methods allow complete recovery of the materials for further analysis. More importantly, literature survey suggests that since the 1990s the number of publications related to solid state NMR and molecular gels are growing in a rapid pace (**Figure 6.1**). Therefore, it is interesting to see how these two co-evolved fields will mutually benefit each other.

6.2 Solid state NMR

6.2.1 Historical perspectives

Historically, while studying the crystalline gypsum ($CaSO_4.2H_2O$), Pake observed a fine structure in the NMR absorption for protons in 1948.[57] His experiments suggested that the NMR spectra from solids has the ability to extract useful structural information and, therefore, can be considered as a complementary tool to X-ray diffraction. This argument was strengthened further, when Andrew *et al*., solved an ambiguity regarding the position of hydrogens in urea using SS NMR spectroscopy.[58] The above experiments have provided a solid foundation to study several inorganic salts and organic crystals using SS NMR. Readers interested in historical development can read various accounts reported in the literature, and a detailed description is beyond the scope of this chapter.[39] In the solid state, anisotropic interactions (i.e., chemical shift anisotropy, dipolar- and quadrupolar interactions) results in broad NMR spectral lines. The dipolar coupling is an inverse cube of the internuclear distance. Therefore, in certain cases, such anisotropic information provides useful insights into the dynamics of specific sites. Where in site specific labelling allows studying the dynamics of the system, interaction sites, and distance constraint. For example, by labelling ^{2}H the one dimensional NMR allows probing dynamis of 10^{-4} to 10^{-7} s, where as multidimensional experiments allow slower motion with a range of 1s.[59] Other nuclei can be used such as ^{13}C or ^{15}N to label and study. However, it is

rather demanding and expensive to prepare isotopically enriched compunds. Therefore, alternative approaches have been utilized. The seminal work by Schaefer and Stejskal in 1976, which combined magic angle (54.74°) spinning (MAS), cross polarization (CP) from proton-to-carbon and high-power proton decoupling commonly known as CP MAS NMR has revolutionized modern SS NMR.[60] The rapid progress in SS NMR has thus opened a new field known as *NMR crystallography* in solid state research, particularly useful for rapid identification of polymorphs and conformational isomers in pharmaceutical industries.[61-62] The term "*NMR crystallography"* was not accepted favourably in early days by the crystallographic community. However, Elena *et al*., clarified the meaning of *NMR crystallography* in a reference foot note in their paper.[63] "*Interestingly, Crystallography is often assimilated today to X-ray studies on single crystals, due to the phenomenal success of this method. Crystallography is obviously a much wider discipline, defined (according to the Encyclopedia Britannica) as "the branch of science that deals with discerning the arrangement and bonding of atoms in crystalline solids and with the geometric structure of crystal lattices." Since the powders we study here are microcrystalline, the term NMR Crystallography appears natural*.

6.2.2 Why solid state NMR of gels?

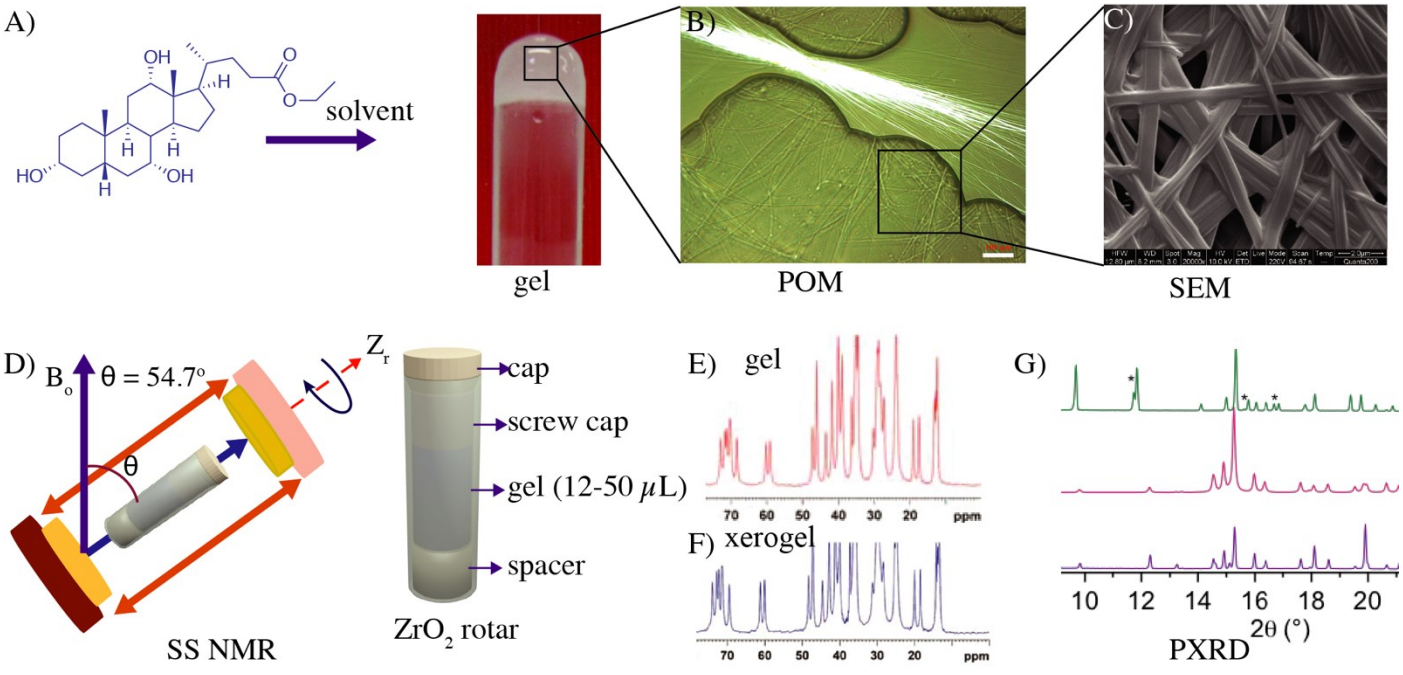

Figure 6.2 Molecular gels and characterization. A) Chemical structure of ethyl cholate and the resulting gel in an aromatic solvent. B) The polarizing optical microscopy image showing the self-assembled fibrillar network. C) SEM micrograph of dried gel. D) Schematic representation of MAS NMR of gel. E&F) ^{13}C CPMAS NMR spectra of a gel and xerogel. G) The powder X-ray powder diffraction patterns.

As discussed in the previous sections, though gels contain a large amount of solvent, they are a self-assembled system (equilibrium or dynamic). Therefore, naturally, there should be some degree of order. Further, electron microscopy studies suggest the presence of nano- or micosized SAFINs depending on the gelator, solvent or conditions (**Figure 6.2**). The rheological studies of many gels show solid-like behaviour in their viscoelastic properties. All the above observations and literature evidence suggests the presence of solid-like aggregates in the gels. Therefore, it is relevant to address whether solid state NMR can be used to obtain relevant information on the nature of the self-assembled superstructures in their native state. Since, liquid state NMR has been well explored to study the free or mobile molecules in the gel network, combining solution NMR with solid state (CP MAS, HR MAS) will provide a better overview on the gels in their native state. In this chapter, we discuss some representative examples from the literature, how SS NMR has been used to study the self-assembled low molecular weight gels and gelators. Further, we discuss how to derive the packing patterns of low molecular weight gelators in their solid and native gel state. NMR crystallography of gels or gelators utilizes a combination of techniques to gain a complete structural detail.

6.3 Solid state NMR of gels

6.3.1 Solid state NMR of polymer gels

Gels (polymeric and low molecular mass) either physical or chemically cross-linked networks are complex viscoelastic materials. The increased viscosity restricts the fast isotropic molecular tumbling or reduces the molecular motion. This also affects the anisotropic interactions like the chemical shift anisotropy (CSA), dipolar- and quadrupolar couplings. As a result, the solution state NMR spectra of gels/viscous liquids display broad signals. Therefore, it is a challenge to extract information related to chemical and structural details. This situation is somewhat similar when solid state NMR experiments are carried out for solids. Nevertheless, the possibility to use SS MAS NMR for gel-like material has been demonstrated by Ford *et al*., in 1985 for polystyrene swollen in $CDCl_3$.[64] Their work showed that ^{13}C MAS NMR spectra of swollen polymer gel could be measured at 4 kHZ spinning frequency. Later, Ginter *et al*., carried out a systematic study of polyethylene oxide (PEO, M_w 3800 Da) hydrogel and compared the solution state and SS MAS NMR (**Figure 6.3A**).[65] In short, the ^{13}C NMR of an aqueous solution of PEO (5wt%), i.e., in its solution state was compared with the ^{13}C MAS NMR and static SS NMR spectra of the gel (70 wt% PEO in water). The spectra in the solid state were measured by placing the gel in a 7 mm (od) zirconia rotor. The ^{13}C MAS NMR was collected at 4 kHz spinning rate, and the ^{13}C resonance patterns of methylene carbon at 69 ppm were compared. The ^{13}C MAS NMR spectra displayed a similar resonance pattern to that of the solution NMR resonance signals. However, broad and overlapping signals were observed in the solid state. This suggests that there are

more than one co-existing phases in the gel state. Authors concluded that this is due to the presence of mobile and immobile components in the gel state.

A more systematic investigation was performed by Kobayashi *et al*. using polyvinyl alcohol (PVA) hydrogel to distinguish the mobile and immobile components (**Figure 6.3B**).[66] In their work, chemical shift values and splitting patterns of ^{13}C signals arising from $–CH_2$ and -CH groups in the solution state, gel state, and solid state were compared. A solution of PVA in D_2O showed splitting into multiplets due to triad and tetrad configurations of –CH and $–CH_2$, respectively.

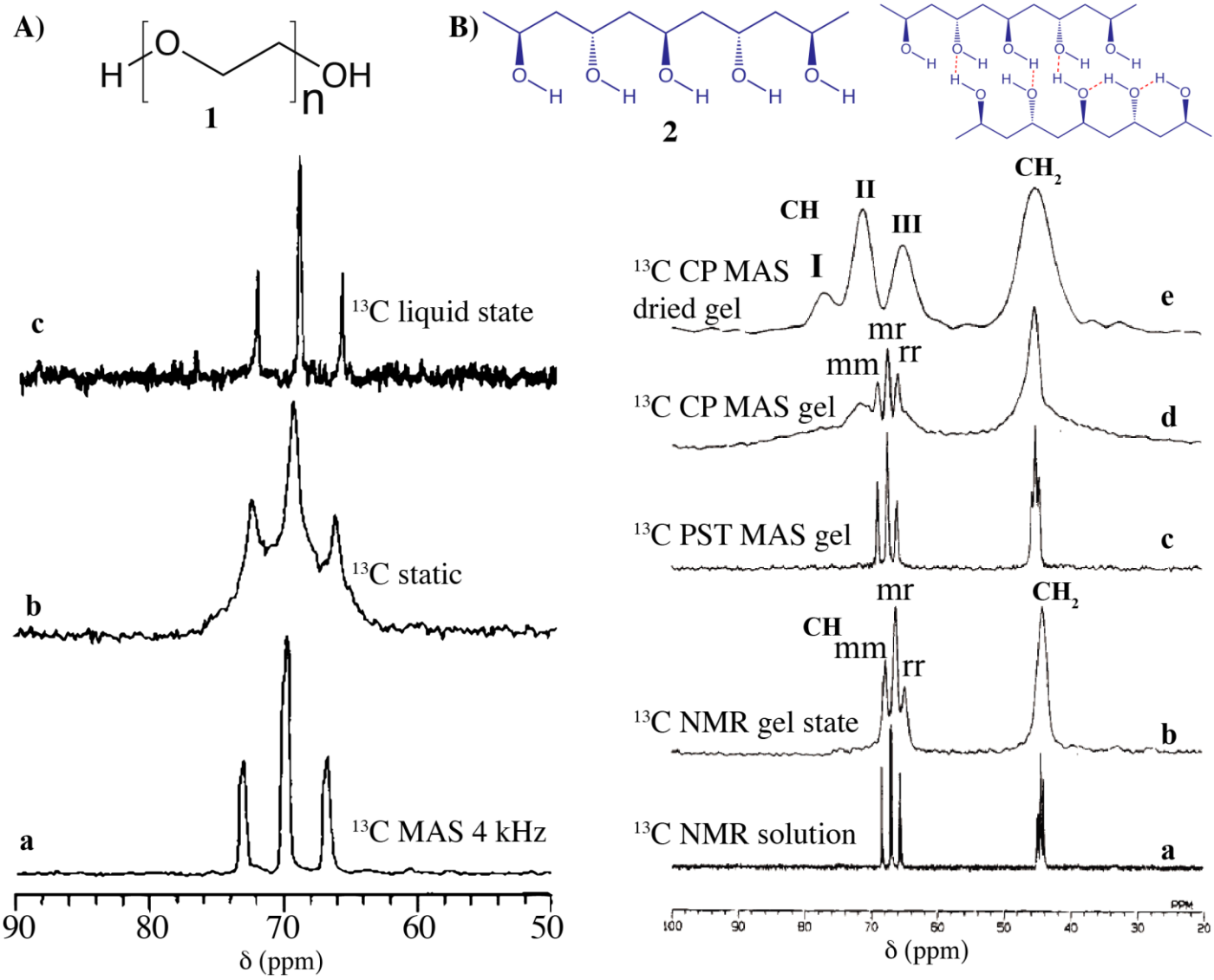

Figure 6.3 Solid state NMR of polymer gels. **A**) comparision of a) ^{13}C MAS NMR spectrum of gel containing 70% PEO and 30% of water at 4 kHz; (b) ^{13}C NMR spectrum of gel containing 70% PEO and 30% of water in a static rotor and (c) ^{13}C NMR spectrum of 5% PEO solution in liquid state probe. Reproduced with permission from ref. 65 © Science Direct. **B**) Chemical structure of polyvinyl alcohol (PVA, **2**) and various hydrogen bonding interaction (a) solution state ^{13}C NMR spectrum of PVA/D_2O solution; (b) solution state ^{13}C NMR spectrum in the gel state; (c) solid state ^{13}C PST MAS

NMR spectrum of the gel; (d) solid state ^{13}C C P MAS NMR spectrum of the gel (e) ^{13}C CPMAS NMR spectrum of the solid. Reproduced with permission from ref. 66 © American Chemical Society

The splitting patterns arising from -CH groups are denoted as *mm, mr* and *rr* (*m* = *meso*, *r*= *racemic*). Interestingly, in the ^{13}C NMR spectrum of gel, –CH shows a triplet and $–CH_2$ showed a broad peak (**Figure 6.3B**). The ^{13}C pulse-saturation transfer (PST) MAS NMR of PVA gels displayed similar spectral features as that of ^{13}C NMR of PVA gel in the solution state. The similarity in the spectral pattern observed under solution state and PST MAS of the gel indicate that in the latter only mobile components are visible. On the other hand, ^{13}C CPMAS NMR spectra of solid PVA the resonance signal from -CH carbon was split into three peaks. Importantly, the chemical shift difference between three peaks was significantly larger compared to those splitting patterns arising from the stereochemical configuration. The splitting of resonance signals of the solid PVA is attributed due to the intramolecular hydrogen bonds between the neighbouring hydroxyl groups within the PVA backbone. The number of hydrogen bonding affects the chemical shift values. Important observations were made by recording the ^{13}C CPMAS NMR of PVA gel, wherein it was found that there are splitting patterns, which resemble the ^{13}C NMR of PVA gel as well as that of the ^{13}C CPMAS NMR of the solid PVA. Furthermore, as the concentration of PVA was increased the ^{13}C CPMAS NMR of the gels tends to display solid-like spectral pattern, and at 35%, the spectra of the gel looked similar to that of the solid PVA. The above examples suggest, that SS NMR of gels can distinguish different components, stereochemical configurations, and the intermolecular interactions. Lai *et al*. carried out a systematic study on the effect of gelation procedure and degree of tacticity in PVA gels using solid state NMR.[67] An extensive discussion on solid state NMR of polymer gels is beyond the scope of this chapter and has been discussed in several literature reports.[68,69] However, the above two examples form the basis for the solution and solid state NMR studies on supramolecular gels. Importantly, for molecular gels the solution state NMR spectroscopy experiments have shown the presence of mobile and immobile as well as the components which are bound to gel network and free molecules.[70] Recently, pulse field gradient (PFG) diffusion ordered NMR spectroscopy (DOSY NMR) experiments and HRMAS studies have been shown to support this hypothesis.[71] The details of such studies have been reviewed elsewhere.[72]. Therefore, the following part of the chapter we will focus towards the solid state NMR of xerogels, aerogels, and native gels with special emphasis on molecular gels.

6.4 Solid state NMR of molecular gels

6.4.1 Solid state NMR of xerogels

One of the early ^{13}C CP MAS studies on xerogel from pseudo-rotaxane formation induced hydrogelation of alkylpyrdinium derivatives in the presence of α-cyclodextrin (α-CD) was reported by Taira *et al* (**Figure 6.4**).[73] The pseudo rotaxane formation was confirmed using MALDI-TOF and NMR spectroscopy. Further, authors used the xerogel derived from a mixture of **3b**:α-CD (1:2) hydrogel to measure the ^{13}C CPMAS NMR spectrum (**Figure 6.4B**). In the ^{13}C CP MAS, spectral resonances arising from C-1 and C-4 carbons of free α-CD that typically appears at signals at 81 and 98 ppm, respectively were absent. This suggests that xerogel is composed of pseudorotaxane. Consequently, the original hydrogel is composed of pseudorotaxane (**Figure 5B**). However, there was no evidence based on solid state NMR of the native gel.

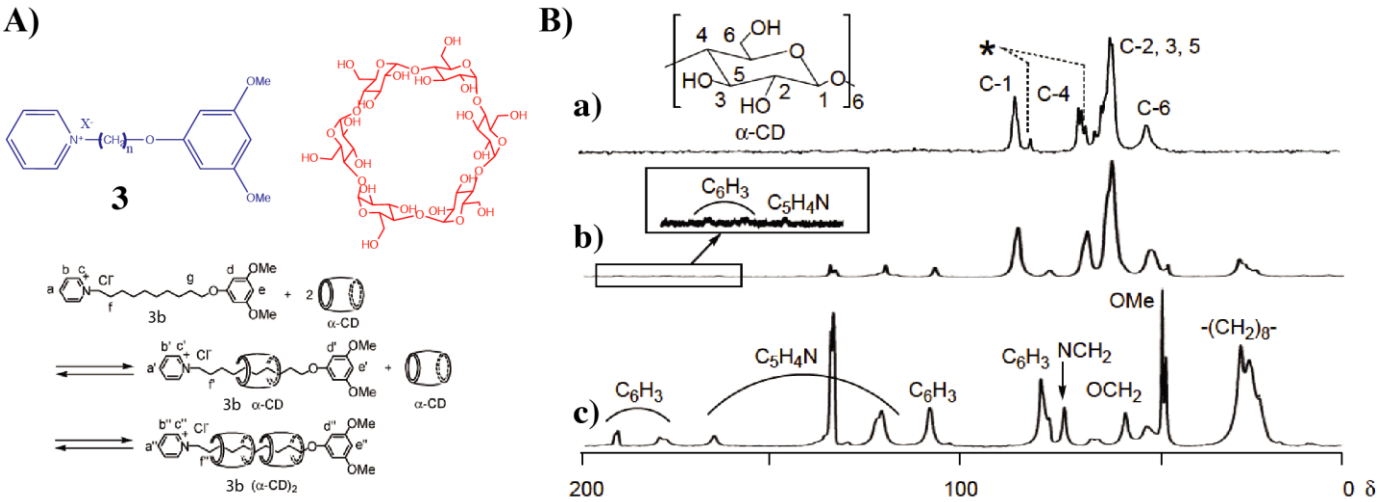

Figure 6.4 Pseudorotaxane based gelators: (**A**) Chemical structures of alkylpyridinium halides and α-cycloderxtrin. (**B**) ^{13}C CPMAS NMR spectra of (a) α-CD; (b) xerogel of **3b** and α-CD, and (c) **3b**. Peaks with an asterisk are assigned to C-1 and C-4 with a conformationally strained glycoside linkage. Reproduced with permission from ref. 73 © Royal Society of Chemistry.

6.4.2 Solid state NMR of gels

One of the first examples for ^{13}C CPMAS NMR of molecular gels was reported by Schoonbeek *et al*., for gels derived from 1,2-bis-urea benzene derivatives in aromatic solvents (**4a-g**, **Figure 6.5A**).[74] They compared the solution ^{13}C NMR, ^{13}C CPMAS NMR of the solid gelator and that of the toluene-d_8 gel (**Figure 6.5B**). The variable concentration ^{13}C NMR in solution state showed no significant changes in the position of ^{13}C resonance peaks. Interestingly, the position of ^{13}C resonances in solution state was also found to be same in ^{13}C CPMAS NMR of the solid gelator and that of toluene-d_8 gel. The observation that the ^{13}C signals did not undergo any change with concentration has been attributed to the presence of strong intra-molecular H-bonding within the gelator molecules as well as strong solute-solvent interaction in the solution. It was suggested that the interactions in the solution state (i.e., a combined intra-molecular and solvent-solute

interactions) essentially have a similar effect as strong inter- and intramolecular interactions in the solid and gel state. Therefore, the position of the resonance peaks remains the same in all three states. Further, the two carbonyls were found to be equivalent in solution, gel state, and solid state. Moreover, the ^{13}C signals arising from aromatic (phenyl) carbons showed no splitting in the solid state NMR. However, the carbons arising from the butyl chains did show splitting. This might be the result of a severe disorder in the flexible alkyl chains. This work did show that ^{13}C CPMAS of molecular gels can be obtained and useful in understanding interactions involved in various forms. However, no clear evidence was obtained from the gel state due to poor spectral resolution.

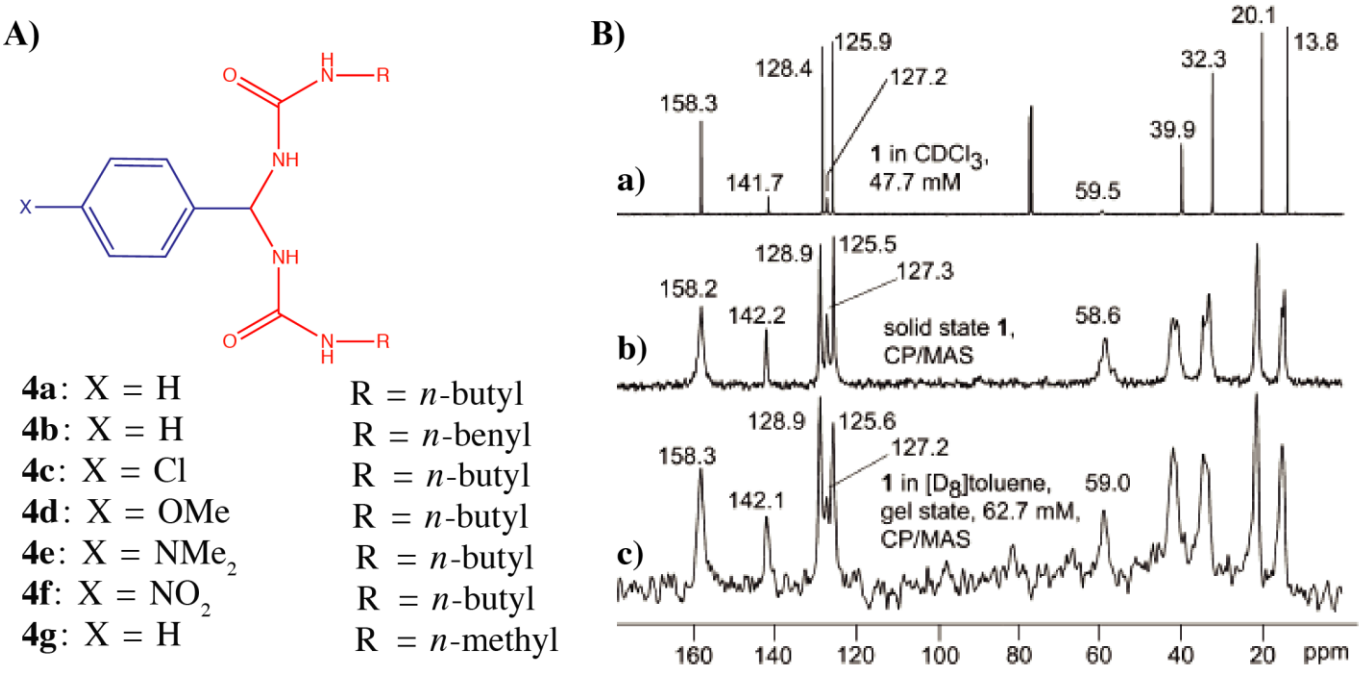

Figure 6.5 Comparison of solution, gel and solid state ^{13}C NMR spectra of **4a**: (a) 47.7 mM in $CDCl_3$; (b) ^{13}C CPMAS NMR of the solid and (c) toluene-d_8 gel of **4a**. Reproduced with permission from ref. 74 © Wiley-VCH.

In 2010, a combined solid state NMR and powder X-ray diffraction of organogels derived from bile acid esters were reported by Nonappa *et al.*[75] More importantly, this study allowed the determination solid state structure of gelator molecules and their packing in gel and xerogel state.[75] This forms the basis for the discussion in the following part of the chapter. Using simple esters of cholic acid, a number of gelators were prepared (**Figure 6.6**).[76] The gel formation was observed only for ethyl, propyl, allyl and propargyl esters of cholic acid. The methyl derivative, readily formed crystals, whereas the butyl derivative, remained in the solution in the tested solvents. The success of this demonstration is due to the choice of the gelators, which have been shown to form highly entangled SAFINs having average lateral dimensions 300 nm and indefinite length. This allowed the direct

observation of the fibers even under the polarizing optical microscope.[77] Moreover, the X-ray powder diffraction patterns of the xerogels also showed high crystallinity, and the fibers were shown to melt at the same temperature as synthetic solid.

First, a comparison of the ^{13}C CPMAS NMR spectra of the synthetic solid and the xerogel was carried out. The synthetic solid, as well as the xerogel samples, displayed identical spectral pattern. Importantly, all the gelators and xerogels displayed doublet resonance pattern, which was a consequence of two non-equivalent molecules present in the asymmetric unit of the crystal lattice. This property has been observed for bile acid itself. The solid state ^{13}C CP MAS NMR spectra were then compared with the native gel state ^{13}C CPMAS NMR, by spinning samples at 4, 5 and 8 kHz. The gels also showed a similar resonance pattern as that of the xerogel and the synthetic solid (**Figure 6.6B**) in their NMR spectra. The identical resonance pattern and the position of the ^{13}C resonances suggest that the packing pattern in the gel state, xerogel, and the solid state are similar.

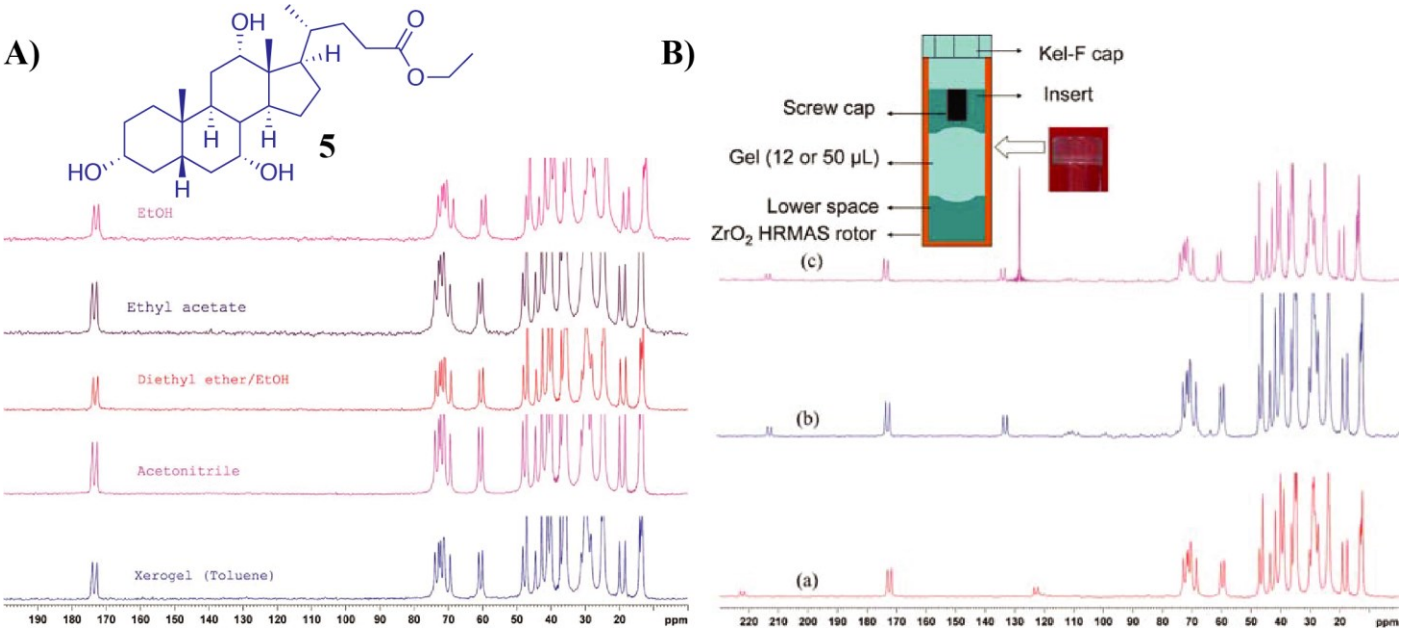

Figure 6.6 Cholic acid ester based gelators: (A) Chemical structure and solid state ^{13}C CPMAS NMR of xerogel and recrystallized samples of ethyl cholate **5** from different solvents. (B) Schematic representation showing the location and preparation of a gel sample for the CPMAS experiment and the ^{13}C CP MAS NMR spectra of benzene-d_6 gel of **5** at (a) 5 kHz and (b) 4 kHz; and (c) benzene gel of **5** at 4 kHz. Reproduced with permission from ref. 75 © Royal Society of Chemistry.

Using powder X-ray powder diffraction indexing and Rietveld refinement, the solid state structure of the gelator was solved. The crystal structure determined using PXRD showed the presence of two non-equivalent molecules in an asymmetric unit of the crystal lattice supporting the the doublet resonance pattern in the ^{13}C CP MAS.

In a related study Noponen *et al*., compared the solid state single crystal X-ray structure, ^{13}C CPMAS NMR and PXRD patterns to understand the packing patterns in the gel state. They used the organogels derived from a series of bile acid–L-methionine methyl ester conjugates (**Figure 6.7**).[78] When recrystallized from acetonitrile, all the conjugates **(6a-c)** formed quality single crystals. However, **6b** and **6c** showed the ability to form organogels in aromatic solvents such as toluene and benzene. A comparision of the solid state ^{13}C CPMAS NMR spectra samples of recrystallized from acetonitrile, with the xerogels and the benzene-d_6 and toluene-d_8 gels was carried out. Interestingly, compound **6c** showed a similar spectral pattern for acetonitrile recrystallized sample and the native gel.

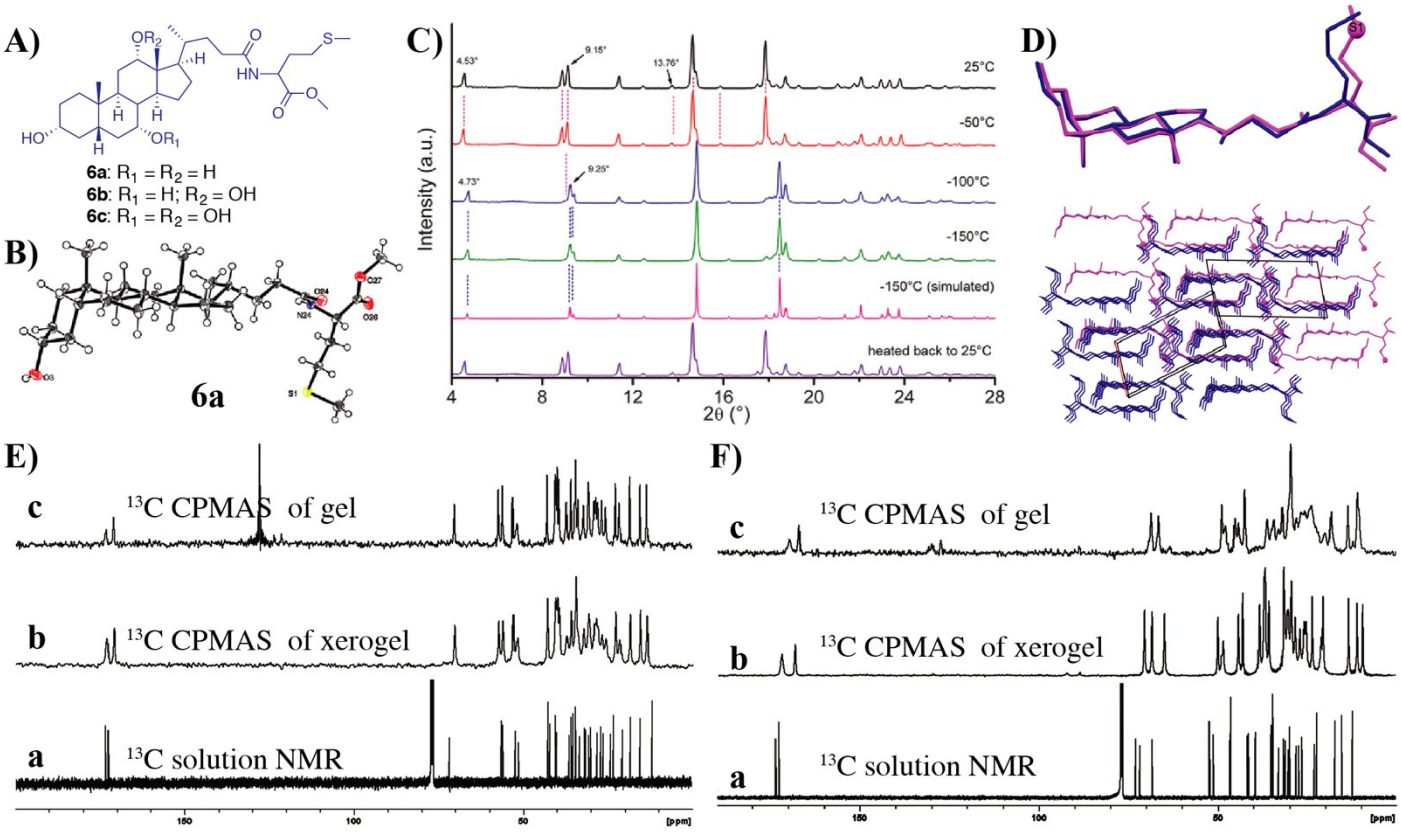

Figure 6.7 Bile acid-methionine ester conjugates. (**A**) Chemical structure of the gelators. (**B**) ORTEP10 plots of asymmetric units of compounds 6a. (**C**) Temperature-dependent diffraction patterns of xerogel of compound 6a together with a simulated pattern of the low-temperature single crystal structure **6a**. (**D**) Overlays of molecular structures (top), and packing modes of single crystal X-ray structure (dark structure) and structure solved using PXRD (light structure) presented along the b-axis of the room-temperature structure **6a**. For clarity, the sulfur atom (S1) of room temperature structure is presented in a ball-style and hydrogen atom. (**E**) ^{13}C NMR spectra of compound **6b**; (a) solution state; (b) ^{13}C CPMAS NMR spectrum of xerogel, (c) ^{13}C CPMAS NMR spectrum of 2% (w/v) benzene gel. (**F**) ^{13}C NMR spectra of compound **6c**; (a) solution state; (b) ^{13}C CPMAS NMR of xerogel and (c) ^{13}C CPMAS NMR spectrum of 4% (w/v) toluene-d_8 gel. Reproduced with permission from ref. 78 © Royal Society of Chemistry.

The above results suggest that the gelator molecules have a similar packing pattern in their gel state and in its crystal structure. Further, a similarity in the PXRD patterns of xerogels and the simulated powder diffraction patterns from single crystal X-ray structure supports that the gel, aerogel and the single crystals have similar packing patterns. On the hand, ^{13}C CPMAS NMR spectral pattern of gels derived from **6b** showed a significant difference from that of the single crystals (**Figure 6.7E**) indicating that the packing patterns in the gel state and single crystals are different.

Ikonen *et al*. studied reported the solid state NMR studies on the gels derived from mono- and diketal derivatives of bile acids.[79] The solid state ^{13}C CPMAS NMR spectra were compared with respective solution state ^{13}C NMR spectra. The monoketal derivatives of pentaerythritol displayed gelation ability in organic solvents (**Figure 6.8**). ^{13}C CPMAS NMR gelator **7a**, recrystallized from toluene, *p*-xylene, and chlorobenzene revealed a doublet resonance pattern indicating the presence of two crystallographically independent molecules per asymmetric unit (**Figure 6.8Bc**). The sample recrystallized from benzene showed the presence of two polymorphic forms. The minor polymorphic form showed similar spectral patterns to those crystallized from other aromatic solvents (**Figure 6.8Bd**) whereas, the major form was found to be a benzene solvate. ^{13}C CP MAS NMR spectra of **7a** recrystallized from acetonitrile or acetone (non-gelling solvents) also showed a doublet resonance pattern. However, the doublet resonance patterns were for the carbons from pentaerythritol moiety were not well resolved, presumably due to severe disorder in that part of the gelator molecule.

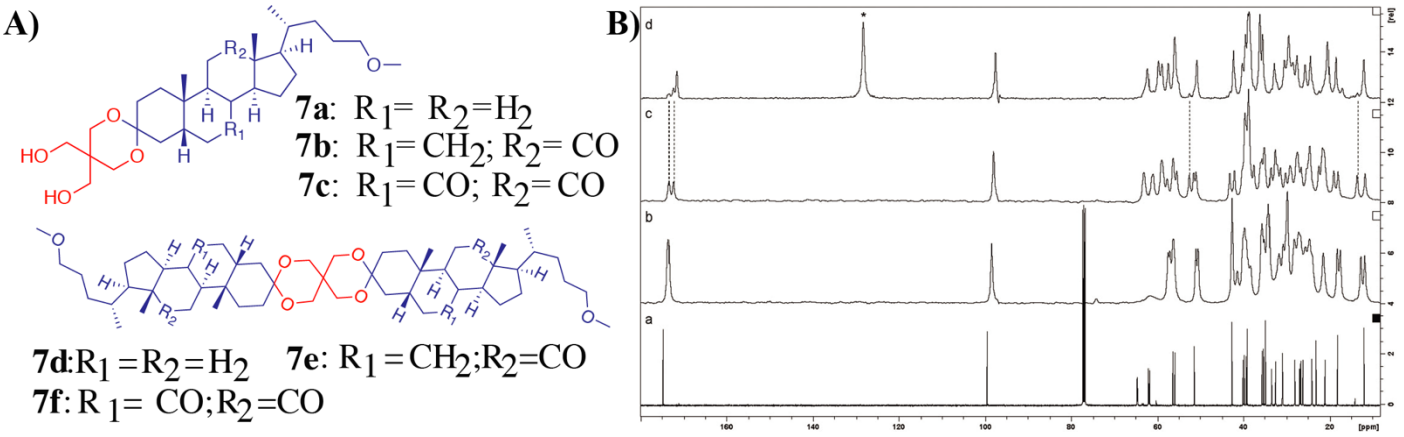

Figure 6.8. A) Chemical structures of monoketal derivatives of bile acids. (**B**) ^{13}C NMR spectrum of **7a** in $CDCl_3$ (a) and ^{13}C CP MAS NMR spectra of **7a** crystallized from acetonitrile (b), toluene (c), and benzene (d). Reproduced with permission from ref. 79 © Royal Society of Chemistry.

Svobodová *et al.*, compared the ^{13}C CPM MAS NMR spectra of synthetic solids, xerogels, and gels derived from stigmasterol-aminoacid conjugates (**Figure 6.9**).[80,81] The ^{13}C CPMAS NMR spectra of of the synthetic solid revealed a certain degree of crystalline, however, relatively broad. However, a systematic analysis of the^{13}C CPMAS NMR spectral data of **8a** revealed three peaks for carbonyl carbon at 169.88, 169.34 and 168.76 ppm. Similarly, in ^{15}N CP MAS NMR, also showed the presence of more than one ^{15}N signals. Therefore, it was concluded that there exists more than one form (i.e., polymorphs). Interestingly, xerogel prepared from the benzene gel of **8a** showed a doublet resonance pattern in its ^{13}C CP MAS NMR (**Figure 6.9Ce**) with carbonyl signals appearing at 169.85 and 168.92 ppm. This suggests, that there are two crystallographically independent molecules in an asymmetric unit of the crystal lattice. Further, it also suggests in the gel state only one polymorphic form exists unlike the synthetic solid. On the otherhand, the ^{13}C CPMAS NMR of CCl_4-gel of **8a** and its xerogel displayed a signlet resonance pattern. This observation further support that the synthetic solid is a mixture of polymorphs and is separated by changing the solvents. On the other hand, 1-butanol gel of **8b** and its xerogels displayed a doublet resonance pattern.

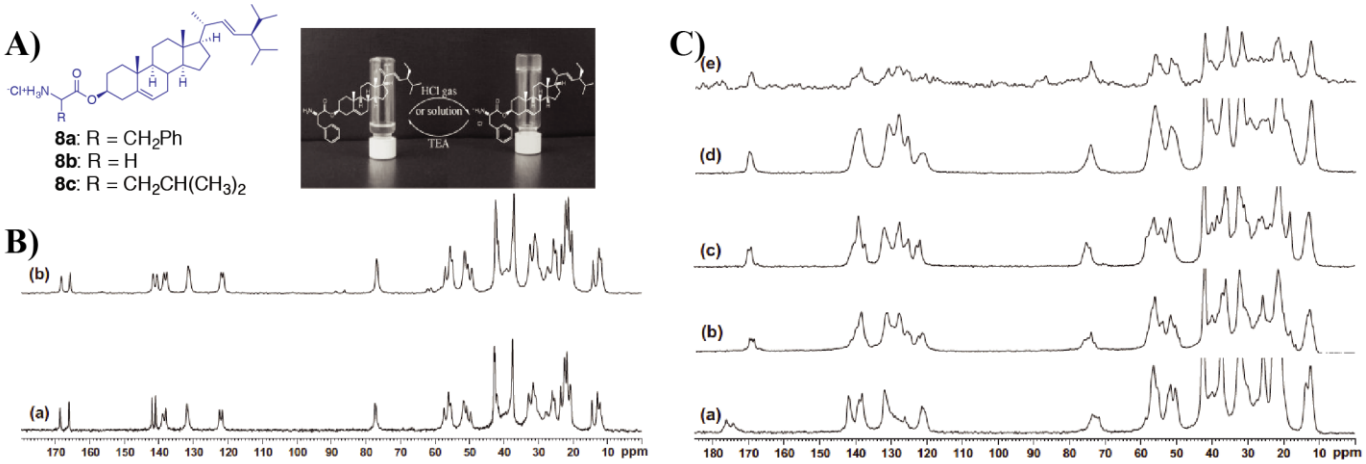

Figure 6.9 (**A**) Chemical structures of stigmasterol-aminoacid conjugates and protonation and deprotonation of stigmasteryl phenylalaninate in tetrachloromethane; (**B**) ^{13}C CPMAS NMR NMR of (a) **8b** solid and (b) xerogel from the 1-butanol gel of **8b**. (**C**) ^{13}C CPMAS NMR of (a) 8a solid; (b) **8b** solid, and xerogels of 8b obtained from (c) benzene gel of **8a**; (d) from CCl_4 gel of **8a**, and (e) CCl_4 gel of **8b** (4% w/v). Reproduced with permission from ref. 80 © Science Direct.

6.4.3 ^{31}P MAS NMR of gels

^{31}P MAS NMR experiments have been used to monitor the thermal transition in phospholipid/cholesterol bilayer systems and to study the effect of cholesterol on phospholipid head group.[82,83] Alanne *et al.*, reported ^{13}C CPMAS and ^{31}P MAS NMR of a gel, xerogel and synthetic solids of bisphosphonate gelators (**Figure 6.10, 9a-d**).[84] Authors suggested that the ^{13}C CPMAS NMR of the synthetic solids and the gels displayed similar spectral patterns, however, they were significantly

different from that of the xerogels. However, in contrast to authors claim, a closer examination of the ^{13}C CPMAS NMR spectra of a synthetic product, xerogel, and gels indicate they all differ significantly, in their spectral patterns. Interestingly, the two ^{13}C CP MAS signals appearing in the gel state shows a resonance signal around 25 ppm similar to that of solid state suggesting that there exists more than one phase in the gel (presumably mobile and immobile components). Further, ^{31}P MAS NMR spectra also revelaed a similar correlation in the spectral patterns as that of ^{13}C CP MAS. ^{31}P MAS NMR spectra of synthetic solid and the xerogels of gelator molecule **9a** were found to be significantly different from each other.

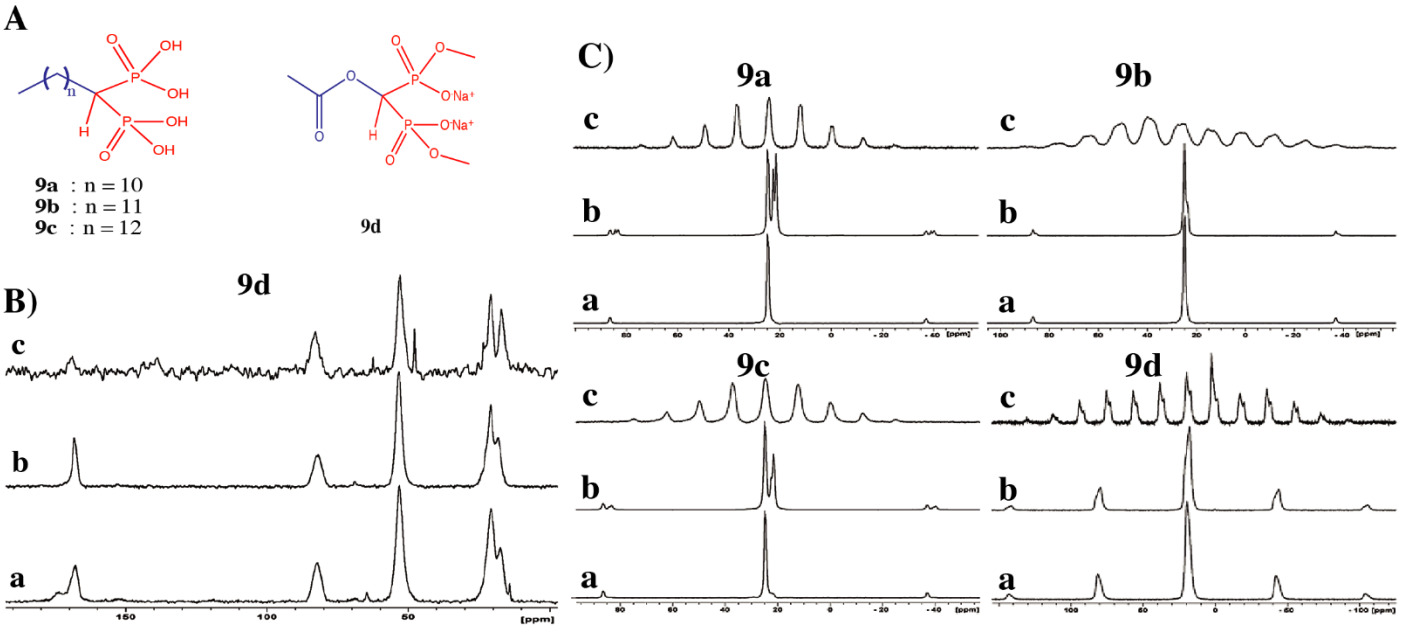

Figure 6.10 Bisphosphonate hydrogelators: (**A**) Chemical structures of hydrogelators; (**B**) ^{13}C CPMAS NMR spectra of (a) synthetic solid; (b) xerogel and (c) gel (4 or 5 w/v%) of **9a** (C) ^{31}P MAS NMR spectra of (a) synthetic solid; (b) xerogel and (c) the hydrogel of **9a-9d**. Reproduced with permission from ref. 84 © Royal Society of Chemistry.

6.4.4 ^{11}B MAS NMR of gels

^{11}B is a spin-3/2 nucleus that produces a strong NMR signal. Further, because of its ability to distinguish between between BO_4 and BO_3 through distinct line shape, ^{11}B MAS NMR has been extensively used to study borosilicate glasses.[85] Borate ester formation has been used to modify the viscosity of various polymers and also to induce gelation of small molecules. ^{11}B MAS NMR is an important tool to study gels but has not been used extensively. Guanosine borate (GB) ester hydrogels have been studied using ^{1}H-decoupled ^{11}B MAS NMR (**Figure 6.11**).[86] The guanosine molecules were treated with various salts such as $KB(OH)_4$ and $CsB(OH)_4$. The K^+ GB gel showed a sharp signal at 11.54 ppm and a small broader shoulder peak at 12.10

ppm. In contrast, the weaker Cs^+ GB gel gave a ^{11}B NMR spectrum with a downfield shifted peak at 13.00 ppm which is larger than the upfield signal at 12.20 ppm. From the above experiments it was suggested that, firstly, ^{11}B NMR signals from borate diesters in the gel and sol states could be resolved by MAS NMR. Secondly, the K^+ GB sample has more borate diester in the gel state than the weaker Cs^+ GB sample.

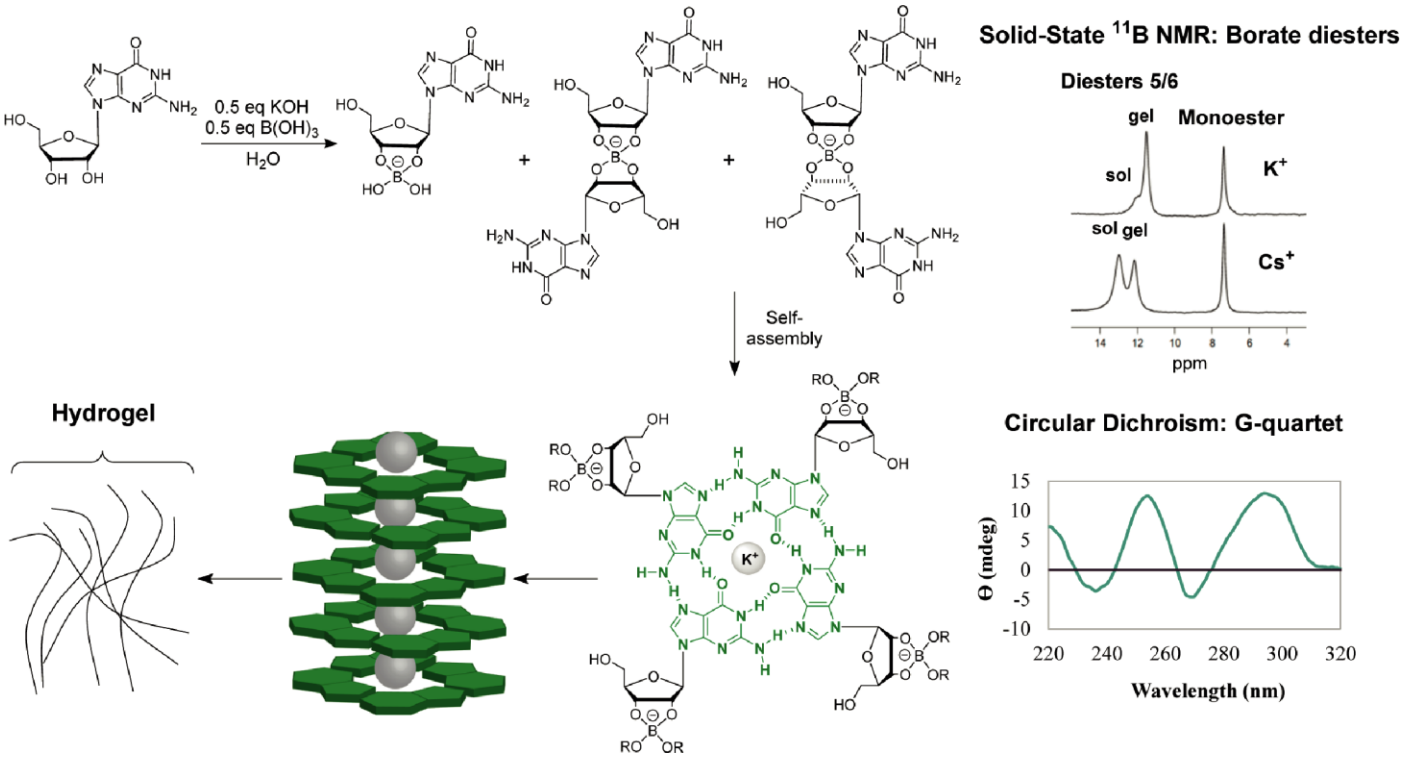

Figure 6.11 Guanasine-borate ester hydrogels. The chemical structure, intermediate and self-assembly mechanism (lef). Solid state ^{11}B MAS NMR of GB gels in the presence of K^+ and Cs^+. Reproduced with permission from ref. 86 under Creative Commons Attribution (CC-BY) License.

6.4.5 2D solid state NMR of gels

One dimensional CP MAS experiments indeed provide valuable information about the packing patterns, the presence of mobile and immobile components or polymorphism within the gel. The study on gels and gelators using solid state NMR is still developing, and there is more scope to extended studies such as 2D solid state NMR spectroscopy. In this context, Nagy-Smith *et al*. used 2D solid state NMR to study the MAX1 peptide hydrogels.[87] MAX1 peptide adopt a β-hairpin conformation which directs the double-layered cross-β structures leading to nanofibrillar networks (**Figure 6.12**). Authors were able to establish a full structural model for the peptide fibrils using SS NMR. In brief, the solid state NMR analyses of the lyophilized sample (i.e., the aerogel) and the sample that was first lyophilized followed by rehydration were compared. The TEM images of the lyophilized sample after rehydration showed similar morphological features as that of the

original hydrogel, indicating that the lyophilization induced artifacts are absent. The peptides were uniformly labelled with ^{15}N and ^{13}C. The 2D ^{13}C-^{13}C solid state correlation NMR spectra showed that a single set of cross-peak signals (**Figure 6.12B**). Further, the lyophilized gels and rehydrated gels showed similar spectral patterns. This ruled out the possibilities of having more than one type of supramolecular structures in the hydrogel (i.e., fibrils are monomorphic) and also suggested that all the peptide molecules are bound to the fiber network (i.e., no free-molecules). To gain structural insights authors have utilized rotational echo double resonance (REDOR) and ^{15}N and ^{13}C backbone recoupling (^{15}N BARE and ^{13}C-BARE) experiments.

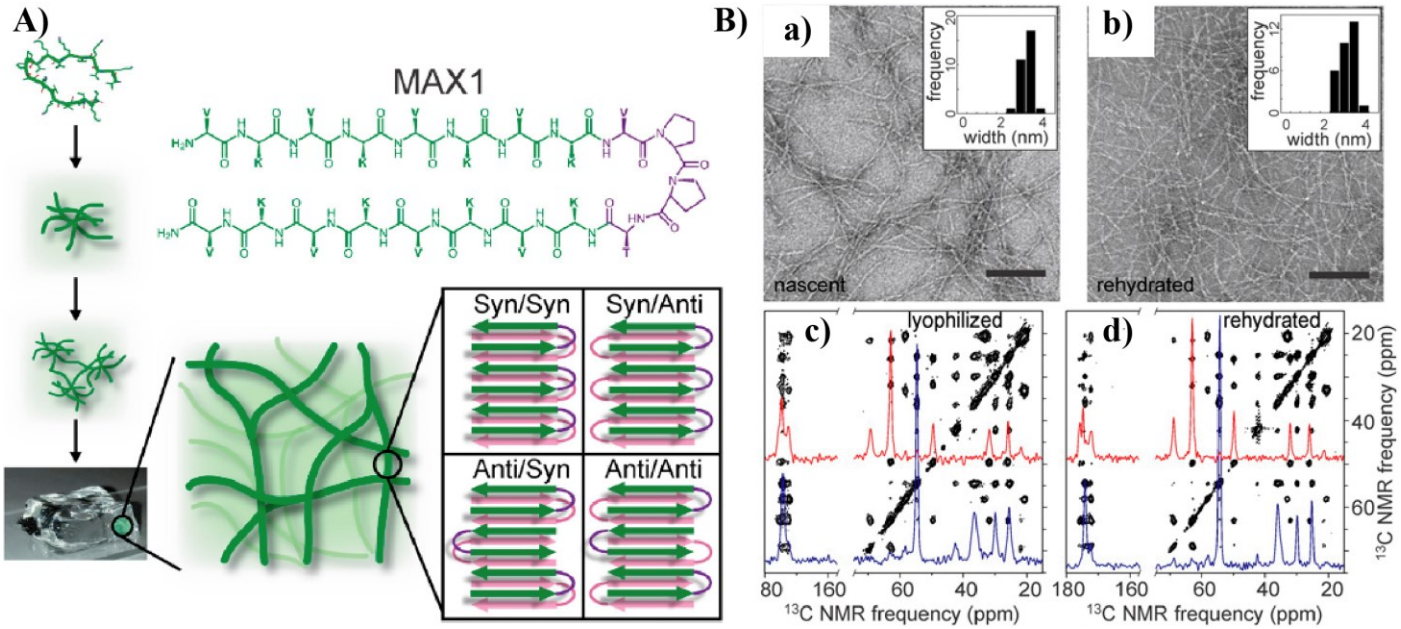

Figure 6.12 (**A**) Self-assembly of MAX1 monomers leads to a hydrogel made from a kinetically trapped network of fibrils, each of which contains a putative double layered β-sheet structure comprised of β-hairpins. Four possible supramolecular structures are shown, differing in the nature of intermolecular alignments within and between the β-sheets. (**B**) Negatively stained TEM images of nascent MAX1 fibrils (**a**) and fibrils in a rehydrated hydrogel after lyophilization (**b**). Two-dimensional solid-state ^{13}C–^{13}C NMR spectra of MAX1 sample IX as a lyophilized gel (**c**) and a rehydrated gel (**d**). One-dimensional slices at Cα chemical shifts of P11 and T12 (red) and K8 and K11 (blue) are shown. Reproduced with permission from ref. 87 © 2015 National Academy of Sciences.

6.4.6 HR MAS of gels

Dried samples of gels have been studied using ^{1}H DQ MAS.[88,89] It has been shown that static ^{1}H multiple quntum (MQ) and HR MAS can be used to study gels in their native state.[90,91] High resolution magic angle spinning (HR MAS) NMR is useful to investigate and compare the mobile and conformationally locked or immobile components in gel phases. Especially, HR MAS is useful to identify the mobile structural moiety that is in grafted to a solid support. When the mobile components show sufficiently high isotropic mobility

with a correlation time of $\leq 10^{-11}$s, due to the elimination of dipolar broadening, sharp signals are obtained. Those moieties that lack the mobility, the low spinning speed used in HR MAS (4 kHz) is not high enough to average dipolar broadening. Therefore the resulting signals are broad and vanish in the noise. Therefore, HR MAS can distinguish between the mobile and immbobile components that are grafted at the interface. Additionally, diffusion filtered (DF) HR MAS can distinguish conformationally mobile moieties and translationally free molecules in the liquid state. The gradient pulsed techniques can encode translationally free diffusing species, but not the grafted ones. Thus the signals arising from the translational motion freedom are suppressed and those without remain unaltered. HR MAS has been used to study the gels derived from valine containing peptide gelators.[91]

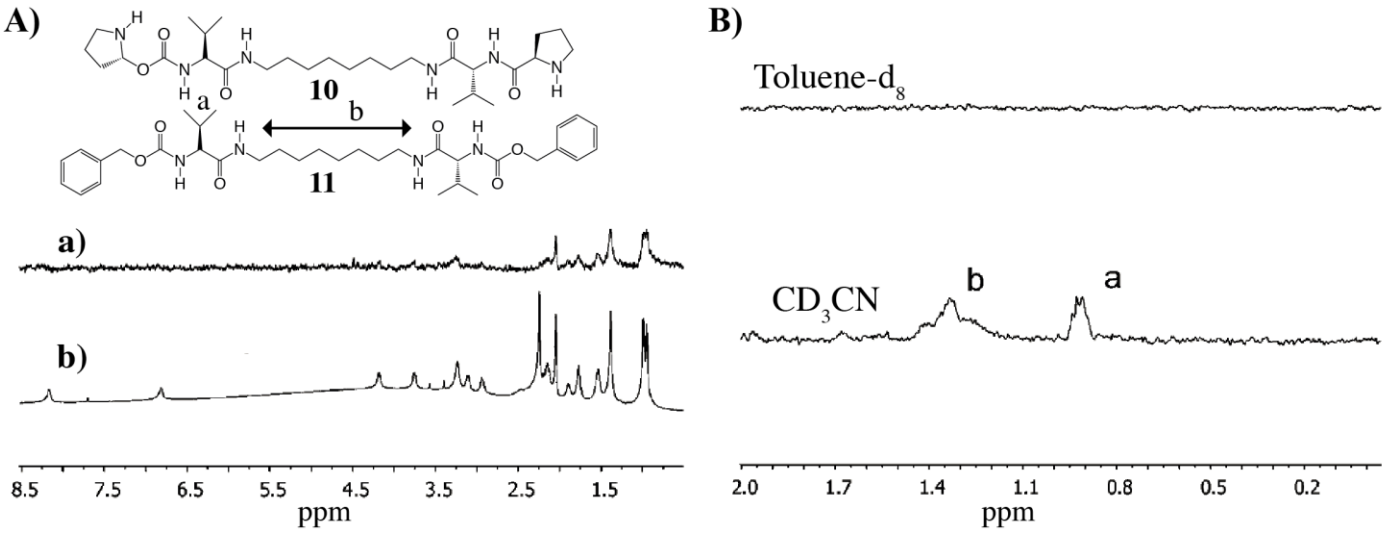

Figure 6.13 (**A**) HR MAS ^{1}H NMR spectra of a gel formed by compound **10** in CD_3CN: (a) no diffusion filter; (b) 50% diffusion filter. (**B**) Diffusion filtered (70%) HR MAS ^{1}HNMRspectra of gels formed by compound **11** in CD^3CN and toluene-d_8. Reproduced with permission from ref. 91 © Royal Society of Chemistry.

It has been shown that when CD_3CN and toluene-d_8 gels of compound (**Figure 6.13**) was measured under HR MAS conditions, significant differences were observed. In CD_3CN gels, the resonances of the valine methyl groups and those of aliphatic briding chains were observed upon applying diffusion filter indicating the rotationally mobile part of those parts. Furthermore, the resonance signals from terminal benzyl groups were not observed presumably due to strong π-stacking. Interestingly, for toluene gel of **10,** no signals were detected under diffusion filtered condition. This suggests stronger agreegates compared to acetonitrile. DF ^{1}H HRMAS of acetonitrile gel by compound **11** showed signals from valine methyl groups and alphatic brigding chain. The toluene gel on the other hand also showed high intense L-proline signals. This suggests the possibily different structural organization in two solvents.

Conclusions

In summary, the continuing interest to study gels has triggered the need for understanding the structure, function, and interactions at different length scales. It is well established that the microscopy is useful to study the nanometric features and X-ray diffraction studies provide ultimate precision in determining the molecular interactions. However, the lack of crystallinity and amorphous nature is a major hurdle in achieving high level details. Therefore, a combination of multiple analytical tools is necessary to gain better insights on gels. In this context, solid state NMR provides valuable information not only about the nature of the packing but also about the various components involved in the native gels. Further, the ability to distinguish mobile and conformationally rigid components allow supporting certain properties of the gels. The recent progress in the field of cryo-TEM and single particle reconstructions offer an additional advantage to gain atomic level details of nanofibers derived from hydrogels, especially from peptides and proteins. Further, there are new techniques such as microelectron diffraction methods have been successfully demonstrated to obtain atomic level 3D structures of small molecules using nanocrystals of organic molecules, which otherwise failed to produce large crystals suitable for X-ray diffraction. Therefore, in future combining solid state NMR of native gels in combination with high resolution electron microscopy, X-ray diffraction, and electron diffraction would result in major advances in understanding the atomic level details of gelators and their interaction at various stages. Solid state NMR is particularly useful to study gels obtained from multicomponent systems.

Acknowledgements

We acknowledge the Academy of Finland´s Centre of Excellence for Molecular Engineering of Biosynthetic Hybrid Materials Research (HYBER) at Aalto University.

References

1. G. M. Whitesides and B. Grzybowski, *Science***,** 2002, **295**, 2418-2421.
2. G. M. Whitesides and M. Boncheva, *Proc. Nat. Acad. Sci*., 2002, **99**, 4769-4774.
3. R. G. Weiss, *Molecular Gels* The Royal Society of Chemistry, 2018.
4. L. A. Estroff and A. D. Hamilton. *Chem. Rev*., 2004, **104**,1201–1218.
5. R. G. Weiss and P. Terech, *Molecular Gels: Materials With Self-Assembled Fibrillar Networks*; Springer, Dordrecht, The Netherlands, 2006, pp. 29.
6. A. R. Hirst, B. Escuder, J. F. Miravet and D. K. Smith, *Angew. Chem. Int. Ed*., 2008, **47**, 8002–8018.
7. P. Terech and R. G. Weiss. *Chem. Rev*.,1997, **97**, 3133–3160.
8. N. M. Sangeetha and U. Maitra, *Chem. Soc. Rev*., 2005, **,**, 821-836.
9. Nonappa., U. Maitra. *Org. Biomol. Chem*., 2008, **6**, 657-669.

10. R. G. Weiss, *J. Am. Chem. Soc*., 2014, **136**, 7519–7530.
11. G. Mieden-gundert, L. Klein, M. Fischer, F. Vögtle, K. Heuzé, J.-L. Pozzo, M. Vallier and F. Fages, *Angew. Chem. Int. Ed*., 2001, **40**, 3164–3166.
12. T. Muraoka, H. Cui and S. I. Stupp, *J. Am. Chem. Soc*., 2008, **130**, 2946–2947.
13. S. Grassi, E. Carretti, L. Dei, C. W. Branham, B. Kahr and R. G. Weiss, *New J. Chem*., 2011, **35**, 445–452.
14. H. Svobodová, V. Noponen, E. Kolehmainen and E. Sievänen, *RSC Adv*., 2012, **2**, 4985–5007.
15. A. E. Hooper, S. R. Kennedy, C. D. Jones and J. W. Steed, *Chem. Commun*., 2016, **52**, 198–201.
16. A. Bertolani, L. Pirrie, L. Stefan, N. Houbenov, J. S. Haataja, L. Catalano, G. Terraneo, G. Giancane, L. Valli, R. Milani, O. Ikkala, G. Resnati and P. Metrangolo, *Nat. Commun*., 2015, **6**, 7574.
17. A. Pizzi, C. Pigliacelli, A. Gori, Nonappa, O. Ikkala, N. Demitri, G. Terraneo, V. Castelletto, I. W. Hamley, F. B. Bombellia and P. Metrangolo, *Nanoscale*, 2017, **9**, 9805-9810.
18. L. Arnedo-Sanchez, Nonappa, S. Bhowmik, S. Hietala, R. Puttreddy, M. Lahtinen, L. DeCola and K. Rissanen, *Dalton Trans*., 2017, **46**, 7309 -7316.
19. R. Tatikonda, E. Bulatov, Z. Özdemir, Nonappa, and M. Haukka, *Soft Matter*, 2019, **15**, 442-451.
20. R. Tatikonda, K. Bertula, Nonappa, S. Hietala, K. Rissanen and M. Haukka, *Dalton Trans*., 2017, **46**, 2793-2802.
21. H. Bunzen, Nonappa, E. Kalenius, S. Hietala and E. Kolehmainen, *Chem. – Eur. J*., 2013, **19**, 12978–12981.
22. H. Wu, J. Zheng, A.-L. Kjøniksen, W. Wang, Y. Zhang, J. Ma, *Adv. Mater*. 2019, **31**, 1806204.
23. D. K. Smith In *Molecular Gels: Structure and Dynamics*, The Royal Society of Chemistry. 2018, pp. 300–371.
24. S. Farrell, D. DiGuiseppi, N. Alvarez and R.Schweitzer-Stenner, *Soft Matter*, 2016,**12**, 6096-6110.
25. I. R. Sasselli, P. J. Halling, R. V. Ulijn and T. Tuttle, *ACS Nano*, 2016, **10**, 2661−2668.
26. I. Kapoor, E.-M. Schön, J. Bachl, D. Kühbeck, C. Cativiela, S. Saha, R. Banerjee, S. Roelens, J. J. Marrero-Tellado and D. D. Díaz. *Soft Matter*, 2012, **8**, 3446-3456.
27. J. D. Hartgerink, E. Beniash, S. I. Stupp, *Science*, 2001, **294**, 1684-1688.
28. L.A. Estroff, L. Leiserowitz, L. Addadi, S. Weiner, A. D. Hamilton, *Adv. Mater*., 2003, **15**, 38-42.
29. G. Zhao, C. Dai, M. Zhao, Q. You, *J. Appl. Polym. Sci*., 2014, DOI: 10.1002/APP.39946.
30. R.Wang. C. Geiger, L. Chen, B. Swanson and D. G: Whitten, *J. Am. Chem. Soc*., 2000, **122**, 2399−2400.

31. G. D. Porta, P. D. Gaudio, F. D. Cicco, R. P. Aquino and E. Reverchon. *Ind. Eng. Chem. Res*., 2013, **52**, 12003–12009.
32. C.A.García-González, M. C. Camino-Rey, M. Alnaief, C. Zetzl and I.Smirnova, *J. of Supercritical Fluids*, 2012, **66**, 297–306.
33. S. L. James, G. O. Lloyd and J. Zhang, *CrystEngComm*, 2015,**17**, 7976-7977.
34. Nonappa, M. Lahtinen, B. Behera, E. Kolehmainen and U. Maitra, *Soft Matter*, 2010, **6**, 1748–1757.
35. P. Terech, E. Ostuni, and R. G. Weiss, *Phys. Chem*., 1996, **100**, 3759–3766.
36. K. Sakurai, Y. Ono, J. H. Jung, S. Okamoto, S. Sakurai and S. Shinkai, *J. Chem. Soc., Perkin Trans*. *2*, 2001, 108–112.
37. J.-H. A.-Larsen, G. S. Boebinger, A. Comment, S. Duckett, A. S. Edison, F. Engelke, C. Griesinger, R. G. Griffin, C. Hilty, H. Maeda, G. Parigi, T. Prisner, E. Ravera, J. Bentum, S. Vega, A. Webb, C. Luchinat, H. Schwalbe and L. Frydman, *Angew.Chem. Int. Ed.,* 2015, **54**, 9162 – 9185.
38. D. I. Freedberg and P. Selenko. *Annu. Rev. Biophys*., 2014, **43**, 171-192.
39. E. R. Andrew, *Bull. Magn. Reson*., 1995, **17**, 16-20.
40. H. Günther, *NMR Spectroscopy: Basic Principles, Concepts and Applications in Chemistry*, 3rd edition by Wiley-VCH: Weinheim, Germany, 2013.
41. M. J. Duer and C. Stourton, *Magn. Reson*., 1995, **17**, 27-36.
42. E. R. Andrew and E. Szczesniak. *Prog. Nucl. Magn. Spec.*, 1995, **28**, 11-36.
43. K.V.R. Chary and G. Govil, *NMR in Biological Systems: From Molecules to Human*, Springer, The Netherlands, 2008.
44. Y. Su, L. Andreas, and R. G. Griffin. *Annu. Rev. Biochem*., 2015, **84**, 465–97.
45. V. Ladizhansky. *Israel J. Chem.*, 2014, **54**, 86-103.
46. K. Wüthrich, *NMR of proteins and nucleic acids*, Wiley-VCH, New York, 1986.
47. M. C. Jarvis and D. C. Apperley, *Plant Physiol*., 1990, **92**, 61–65.
48. A. Alia, S, Ganapathy and H. J. M. de Groot, *Photosynth*. *Res*., 2009, **102**, 415–425.
49. X. L. Warnet, A. A. Arnold, I. Marcotte, and D. E. Warschawski*, Biophys. J.* 2015, **109**, 2461–2466.
50. R. W. Vaughan. *Annu. Rev. Phys. Chem*., 1978, **29**, 397-419.
51. T. Charpentier, *Solid State Nucl. Magn. Reson.* 2011, **40**, 1-20.
52. A. Sutrisno and Y. Huang, *Solid State Nucl. Magn. Reson.,* 2013, **49**, 1-11.
53. R. K. Harris, *Analyst*, 2006, **131**, 351 – 373; R. K. Harris, In *Encyclopedia of Nuclear Magnetic Resonance*, Ed. D. M. Grant and R. K. Harris, Wiley, Chichester, 1996, pp 3734 – 3740.

54. D. D. Laws, H.-M. L. Bitter and A. Jerschow, *Angew. Chem. Int. Ed*., 2002, **41**, 3096–3129.
55. C. Dybowski and S. Bai, *Anal. Chem*., 2008, **80**, 4295–4300.
56. Nonappa, M. Lahtinen, S. Ikonen, E. Kolehmainen and R. Kauppinen., *Cryst. Growth Des*., 2009, **9**, 4710–4719.
57. G. E. Pake, *J. Chem. Phy*., 1948, **16**, 327-3367.
58. E. R. Andrew and D. Hyndman, *Faraday Sot. Discuss.*, 1955,**19**, 195.
59. S. P. Brown and H. W. Spiess, *Chem. Rev*. 2001, **101**, 4125-4155.
60. J. Schaefer and E. O. Stejskal, *J. Am. Chem. Soc*., 1976, **98**, 2013.
61. R. K. Harris. *Solid State Sci*., 2004, **6**, 1025–1037;
62. *NMR Crystallography*, Ed. R. K. Harris, R. D. Wasylishen and M. J. Duer, John Wiley & Sons Ltd, Chichester, 2009.
63. B. Elena, G. Pintacuda, N. Mifsud and L. Emsley, *J. Am. Chem. Soc*., 2006, **128**, 9555-9560.
64. W. T. Ford, S. Mohganraj, H. Hall and D. J. O´Donnell, *J. Magn. Reson*., 1985, **65**, 156.
65. D. M. Ginter, A. T. Bell and C. J. Radke. *J. Magn. Reson*., 1989, **81**, 217-219.
66. M. Kobayashi, I. Ando, T. Ishiif and S. Amiya, *Macromolecules*, 1995, **28**, 6677-6679.
67. S. Lai, M. Casu, G. Saba, A. Lai, I. Husu, G. Masci and V. Crescenzi, *Solid State Nuclear Magn. Res.* 2002, **21**, 187-196.
68. H.Yasunaga, M. Kobayashi, S. Matsukawa, H. Kurosu and I. Ando, *Ann. Rev. NMR Spectroscopy*, 1997, **34**, 39-104.
69. M. E. Smith and D. Holland, *Atomic-Scale Structure of Gel Materials by Solid-State NMR BT - Handbook of Sol-Gel Science and Technology*. In L. Klein, M. Aparicio and A. Jitianu (Eds.) Cham: Springer International Publishing. 2016, pp. 1–43.
70. B. Escuder, M. Llusar and J. F. Miravet, *J. Org. Chem*., 2006, **71**, 7747 – 7752.
71. Nonappa, D. Šaman and E. Kolehmainen, *Magn. Reson. Chem*., 2015, **53**, 256-260.
72. G. Yu, X. Yan, C. Han and F. Huang, *Chem. Soc. Rev*., 2013, **42**, 6697.
73. T. Taira, Y. Suzaki and K. Osakada, *Chem. Commun*., 2009, 7027–7029.

74. F. S. Schoonbeek, J. H. van Esch, R. Hulst, R. M. Kellogg and B. L. Feringa, *Chem. Eur. J.,* 2000, **14**, 2633-2643.

75. Nonappa, M. Lahtinen, B. Behera, E. Kolehmainen and U. Maitra, *Soft Matter*, 2010, **6**, 1748–1757.

76. Nonappa and U. Maitra, *Soft Matter*, 2007, **3**,1428-1433.

77. Nonappa and E. Kolehmainen, *Soft Matter*, 2016,**12**, 6015-6026.

78. V. Noponen, Nonappa, M. Lahtinen, A. Valkonen, H. Salo, E. Kolehmainen and E. Sievänen, *Soft Matter*, 2010, **6**, 3789–3796.

79. S. Ikonen, Nonappa, A. Valkonen, R. Juvonen, H. Salo and E. Kolehmainen, *Org. Biomol. Chem*., 2010, **8**, 2784–2794.

80. H. Svobodová, Nonappa, Z. Wimmer, E. Kolehmainen, *J. Colloid Interface Sci*., 2011, **361**. 587–593.

81. H. Svobodová, Nonappa, M. Lahtinen, Z. Wimmer and E. Kolehmainen, *Soft Matter*, 2012, **8**, 7840.

82. W. Guo, V. Kurze, T. Huber, N. H. Afdhal, K. Beyer, J. A. Hamilton, *Biophys. J.,* 2002, **83**, 1465-1478.

83. A. L. Costello and T. M. Alam. *Biochim. Biophys. Acta - Biomembranes* 2008, **1778**, 97-104.

84. A.-L. Alanne, M. Lahtinen, M. Löfman, P. Turhanen, E. Kolehmainen, J. Vepsäläinen and E. Sievänen, *J. Mater. Chem. B*, 2013, **1**, 6201.

85. M. A. Villegas, J. Sanz and J. M. Navarro, *J. Non-Cryst Solids*, 1990,**121**, 171.

86. G. M. Peters, L. P. Skala, T. N. Plank, B. J. Hyman, G. N. M. Reddy, A. Marsh, S. P. Brown and J. T. Davis, *J. Am. Chem. Soc*., 2014, **136**, 12596-12599.

87. K. Nagy-Smitha, E. Moorec, J. Schneidera and R. Tycko, *Proc. Nat. Acad. Sci*., 2015, **112**, 9816–9821.

88. S. P. Brown, *Curr. Opinion Colloid & Interface Sci*., 2018, **33**, 86-98.

89. E. Diez-Pena, I. Quijada-Garrido, J.M. Barrales-Rienda, I. Schnell and H.W. Spiess, *Macromol. Chem, Phys.*, 2004, **205**, 430-437.

90. F. Lange, K. Schwenke, M. Kurakazu, Y. Akagi, U.I. Chung and M. Lang. *Macromolecules*, 2011, **44**, 9666-9674.

91. P. Shestakova, R. Willem and E. Vassileva*, Chem. -A Eur. J.*, 2011, 17, 14867-14877.

92. S. Iqbal, F. R.-LLansola, B. Escuder, J. F. Miravet, I. Verbruggenb and R. Willem, *Soft Matter*, 2010, **6**, 1875–1878.